ChemMedChem

Chemistry Europe
European Chemical Societies Publishing
ChemMedChem

RESEARCH ARTICLE

Synthesis and Evaluation of Iminosugar-Based Analogs of UDP-GlcNAc as Putative OGT Inhibitors

Nicolas Auberger[1] | Thanh Van Tran[1] | Quentin Lemaire[2] | Jil Busmann[3] | Marine Lacritick[4] | Marlène Mortuaire[2] | Céline Schulz[2] | Anne-Sophie Vercoutter-Edouart[2] | Arnaud Pâris[5] | David Vocadlo[3] | Pierre Lafite[5] | Stéphane P. Vincent[4] | Tony Lefebvre[2] | Yves Blériot[1]

[1]Glycochemistry Group, OrgaSynth Team, IC2MP, UMR CNRS, 7285, Université de Poitiers, Poitiers cedex 09, France | [2]Unité de Glycobiologie Structurale et Fonctionnelle (UGSF), CNRS, Université de Lille (UMR 8576), Lille, France | [3]Department of Chemistry, Simon Fraser University, Burnaby, British Columbia, Canada | [4]Département de Chimie, Laboratoire de Chimie Bio-Organique, University of Namur, Namur, Belgium | [5]Institute of Organic and Analytical Chemistry (ICOA), UMR, 7311, CNRS-Université d 'Orléans, Université d'Orléans, Orléans Cedex 2, France

Correspondence: Pierre Lafite (pierre.lafite@univ-orleans.fr) | Stéphane P. Vincent (stephane.vincent@unamur.be) | Tony Lefebvre (tony.lefebvre@univ-lille.fr) | Yves Blériot (yves.bleriot@univ-poitiers.fr)

Received: 12 February 2026 | **Revised:** 27 May 2026 | **Accepted:** 24 June 2026

Keywords: glycoconjugate | glycosyl transferase | iminosugar | OGT

ABSTRACT

O-GlcNAc transferase (OGT) is an essential mammalian enzyme that regulates numerous cellular processes through the attachment of *O*-linked *N*-acetylglucosamine (*O*-GlcNAc) residues to nuclear and cytoplasmic proteins. Inhibitors of OGT are needed as research tools and for evaluating the potential of OGT as a therapeutic target. As little effort has been made to incorporate mimicry of the glycosyl oxocarbenium character of the OGT transition state, we report herein the synthesis of a series of glycomimetics of the OGT substrate UDP-GlcNAc, in which the GlcNAc motif has been replaced by an imino-*C*-glycoside and the pyrophosphate moiety has been either conserved, replaced by a squaramide linker, or truncated to remove the terminal phosphate and base. While their affinity for human OGT both in vitro and in cells proved modest (>300 μM), an imino-*C*-glycoside of α-D-GalNAc-1-phosphate showed, surprisingly, micromolar noncompetitive inhibition of OGT (IC_{50} = 50 μM).

1 | Introduction

Glycosyltransferases are ubiquitous enzymes that have vital cellular roles in organisms found in all kingdoms of life. These enzymes catalyze transfer of a sugar from a donor, most commonly a nucleotide sugar, to a variety of proteins [1]. One glycosyltransferase that has received considerable recent attention is human *O*-GlcNAc transferase (hOGT) [2]. hOGT transfers *N*-acetylglucosamine from the sugar donor UDP-GlcNAc onto specific serine or threonine residues of a wide variety of nuclear, mitochondrial, and cytoplasmic proteins with inversion of the configuration at the anomeric center [3]. The client proteins include transcription factors, cytoskeletal proteins, enzymes, kinases, phosphatases, proteasome components, and chaperones proteins [4]. This dynamic post-translational modification, counterbalanced by the activity of a corresponding glycosidase, *O*-GlcNAcase (OGA), which removes GlcNAc residues from proteins [5], is highly conserved in a wide range of organisms and is now recognized as an important regulatory form of glycosylation within cells. The balanced activity of the two enzymes OGT and OGA controls *O*-GlcNAc cycle, its deregulation being implicated in various metabolic disorders such as diabetes, cancers, cardiovascular diseases, obesity, and neurodegeneration [6]. Major questions in regard to the function of OGT include how the specificity of the enzyme is determined [7], as OGT has numerous diverse substrates, and how the UDP-sugar binds and is transferred. While the overall mechanism of OGT has been elucidated (Figure 1a) [8], the nature of the catalytic base deprotonating serine residue is still uncertain [9, 10]. Catalysis by OGT involves formation of a ternary substrate complex with UDP and a polypeptide, which then leads to glycosyltransfer occurring through a transition state with high oxocarbenium character at the sugar moiety.

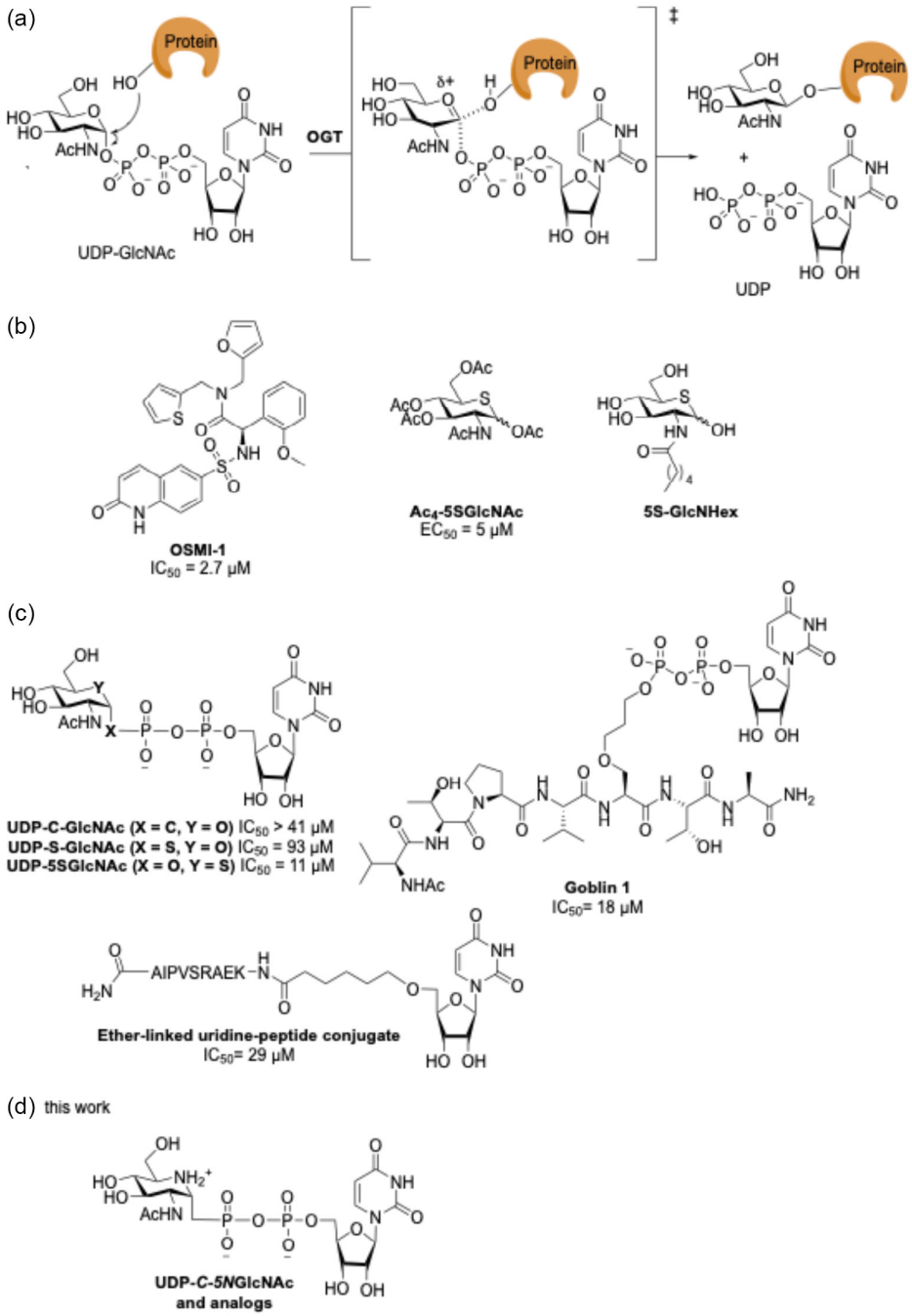

FIGURE 1 | (a) Putative mechanism of OGT; (b) Potent OGT inhibitors; (c) bisubstrate analog OGT inhibitors; and (d) this work.

Due to the biological importance of OGT, a considerable set of inhibitors has been reported [11]. Both high throughput screening and rational design, exploiting understanding of the mechanism and structure of OGT, have led to identification of fairly potent cell active OGT inhibitors, including OSMI-1 [12], a substrate-derived polypeptide [13], Ac_4-5SGlcNAc [14] and its derivative 5S-GlcNHex [15]. These latter two compounds both hijack the hexosamine biosynthetic pathway, which is the metabolic pathway through which UDP-GlcNAc is biosynthesized (Figure 1b). Knowledge of the ternary complex has been also exploited to design bisubstrate analog inhibitors, with various combinations of UDP-peptide conjugates having been examined [16, 17] including "Goblin 1" as an example. The pyrophosphate linkage has been also replaced by more robust tethers [18]. We noted, however, that in all of these substrate and bisubstrate mimics, there have not been efforts made to incorporate mimicry of the glycosyl oxocarbenium character of the OGT transition state [19]. We reasoned that design of UDP-sugar conjugates in which the GlcNAc sugar moiety is replaced by the corresponding iminosugar [20], which is protonated at physiological pH, might lead to OGT inhibition and bring valuable information about the structural requirements for inhibition of this key glycosyltransferase. Following on this line of reasoning, a vast array of iminosugars has been previously reported as glycosyltransferases inhibitors [21], some of which provide insights into enzyme catalysis.

2 | Results and Discussion

2.1 | Synthesis of Glycomimetics

Several UDP-GlcNAc analogs have been reported as OGT inhibitors including UDP-*C*-GlcNAc [22], UDP-*S*-GlcNAc [23], and UDP-*5S*GlcNAc [14] (Figure 1c). However, the corresponding imino-*C*-glycoside, UDP-*C*-*5N*GlcNAc and its derivatives have, to the best of our knowledge, not been described and are worth investigating. Only three GDP-iminosugars and analogs have been reported in the literature [24–26] that were assembled using either the morpholidate [27] or the carbonyldiimidazole (CDI) method [28]. We have previously reported the synthesis of imino-*C*-GlcNAc and imino-*C*-GalNAc phosphonates **1** and **2** [29]. To access UDP-*C*-*5N*GlcNAc and analogs, these two molecules were treated with TMSI to afford the fully deprotected iminosugar phosphonates **3** and **4** (Scheme 1). The GalNAc-configured derivative **4** was used as a negative control. We then attempted to couple GlcNAc derivative **3** either to UMP-morpholidate using standard conditions or to UMP using CDI [25], however, all efforts led to intractable reaction product mixtures (data not shown). We thus applied the coupling method developed by Jemielty et al. [30, 31] using uridine-5′-phosphorimidazolide and a stoichiometric amount of $MgCl_2$ in *N*, *N*-dimethylformamide (DMF) [32]. This method is generally quicker than morpholidate coupling (reaction time of 20 h as opposed to 3–4 days) and requires a lower excess of activated UMP, thus facilitating the purification step by lowering the amount of side-products (mainly UMP and UppU, the dimer of UMP). The target UDP-*C*-*5N*GlcNAc **5** was purified by reverse-phase HPLC and its structure was ascertained by ^{1}H-, ^{13}C-, ^{31}P-NMR, and by HRMS (Supporting Information). The modest yield (10%) is mainly ascribed to the challenging purification of the final molecule.

To possibly improve the overall yield of this coupling reaction, we briefly examined the enzymatic synthesis of UDP-*C*-*5N*GlcNAc **5** from iminosugar phosphonate **3** (Figure S3). To the best of our knowledge, such coupling involving UTP and iminosugar derivative has not been reported and could open perspectives for the synthesis of innovative glycoconjugates.

We concede that, while the pyrophosphate unit in these molecules may confer an increase in potency, these compounds would have a low permeation level into cells. In addition, the pyrophosphate group might limit physiological stability. The squaramide functionality has been identified as a pyrophosphate bio-isostere and used to develop uridine-peptide conjugates as OGT inhibitors [16]. We therefore incorporated squaramide in a new UDP-GlcNAc analog **6**, exploiting the known azide-derivatized iminosugar **7** [25]. The free amine of compound **7** was *N*-benzylated under standard conditions to afford fully protected iminosugar **8** in 85% yield which azido group was reduced (H_2, Pd/C, CH_3OH), yielding the crude amine **8′** (Scheme 2). In parallel, squaramide **10** was obtained in 83% yield from known amino-uridine **9** [16] through treatment with 3,4-diethoxy-cyclobutene-1,2-dione in the presence of *N*, *N*-diisopropylethylamine (DIPEA) in ethanol. Coupling of the crude amine **8′** with squaramide **10** in the presence of DIPEA afforded iminoglycoconjugate **11** in 78% yield. Removal of the acetonide group under acidic conditions provided diol **6** in 84% yield. Benzyl group removal was then examined. Unfortunately, use of classical conditions such as hydrogenolysis ($Pd(OH)_2$, H_2, 1 atm, HCl, iPrOH, 48 h at rt) [33] of **6** or treatment with BCl_3 (12 eq.) in dichloromethane at low temperature (–78 °C to rt) [34] furnished an inseparable mixture of partially deprotected compounds. As a partially protected five-membered iminosugar-derived UDP-GlcNAc glycomimetic, in which the β-phosphate has been replaced by either an alkyl chain or a triazolyl ring, has been previously reported to inhibit OGT in the micromolar range [35], we were encouraged to assay compound **6**.

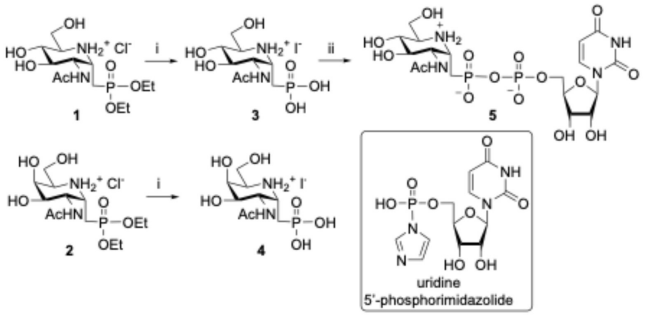

SCHEME 1 | Chemical synthesis of imino-*C*-glycosides **3–5**: (i) TMSI, CH_2Cl_2, 77%; (ii) uridine-5′-phosphorimidazolide, $MgCl_2$, DMF, 10%.

2.2 | Enzymatic Studies with Human OGT In Vitro

The four synthesized imino-*C*-glycosides **3**-**6** were evaluated as inhibitors of human OGT in vitro (Table 1; Figure S1). These compounds were first assayed at a concentration of 50 µM and the extent of inhibition was measured. This 50 µM concentration was selected as a first-pass criterion since it facilitates the detection of genuine inhibitors rather than compounds having indirect effects on the OGT activity. This initial assay revealed that most compounds showed little inhibition, even at 50 µM. Nevertheless,

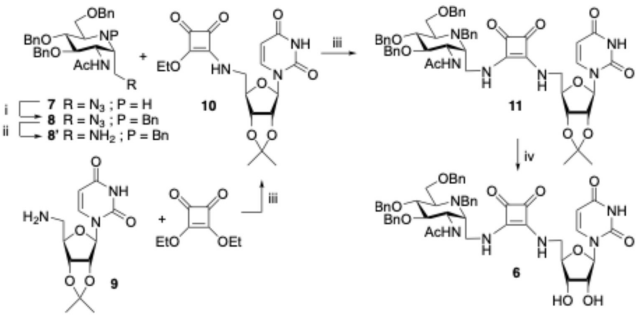

SCHEME 2 | Synthesis of UDP-*C*-GlcNAc analog **6**; (i) BnBr, $KHCO_3$, $AcOEt/H_2O$, 85%; (ii) H_2, 10% Pd/C, MeOH; (iii) DIPEA, EtOH, 83% for **10**, 78% for **11**; (iv) TFA, H_2O, THF, 84%.

TABLE 1 | Enzymatic inhibition of hOGT.

Analog	Cpd	IC_{50} (µM)	Type of inhibition
GlcNAc-P	**3**	333	ND
GalNAc-P	**4**	48	Noncompetitive
UDP-GlcNAc	**5**	407	ND
UDP-GlcNAc	**6**	700	ND

ND: Not determined due to weak binding.

three analogs (**3**, **4,** and **5**) showed greater than 10% inhibition of hOGT suggesting that these could be legitimate OGT inhibitors and therefore these compounds were selected for further study. UDP-*C*-*5N*GlcNAc **5** is an analog of UDP-*C*-GlcNAc in which the sugar endocyclic oxygen has been replaced by nitrogen. This small structural change has a surprisingly dramatic effect on inhibition as the potency of **5** (IC_{50} 407 μM) is about 10 times lower than its oxygenated counterpart (IC_{50} ~ 40 μM). Similarly weak inhibition is observed when using **3**, which lacks the UMP moiety, suggesting that the iminosugar moiety, probably protonated under assay conditions, seems to hinder binding within the OGT active site - leading to poor inhibition.

Interestingly, UDP-*C*-GlcNAc analog **6**, in which the β-phosphate of the pyrophosphate linkage has been replaced by a squaramide weakly inhibits hOGT (IC_{50} 700 μM) despite its partial protection, a phenomenon previously observed with fully protected polyhydroxylated pyrrolidines [35]. Surprisingly, the most potent compound is the GalNAc-configured analog **4** (IC_{50} 48 μM). To gain insight into its inhibition mode, we set up a FP assay (Figure S2). When incubating OGT with the fluorescently labeled nucleotide sugar (UDP-GlcN-BODIPY), the addition of UDP as a competitor leads to decreased fluorescence polarization, indicating that UDP is competing with UDP-GlcN-BODIPY for binding to the active site. In contrast, the addition of **4** did not increase polarization even at 1 mM, suggesting that **4** is not competing with UDP-GlcN-BODIPY for binding to the active site of OGT. This observation suggests that **4** is not an active site binder but rather an allosteric OGT inhibitor, of which only one other is known to our best knowledge [36].

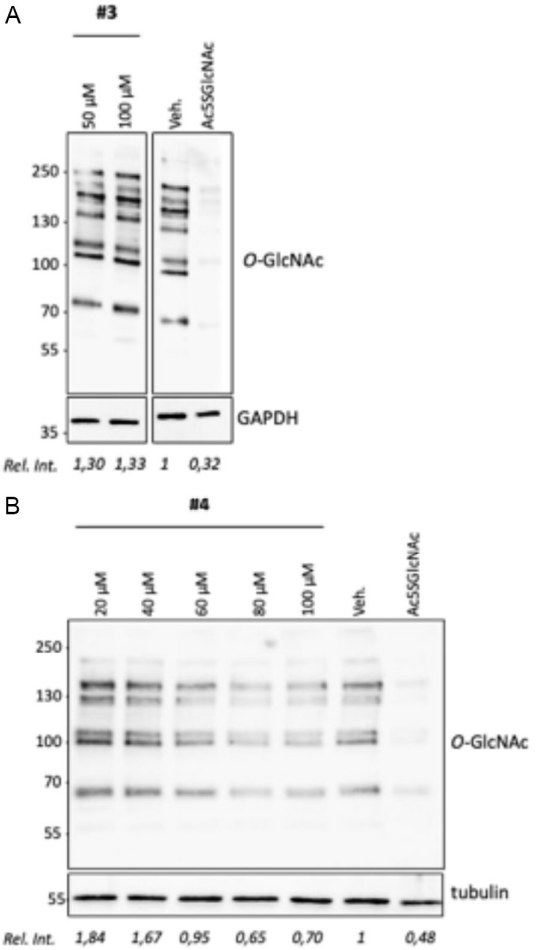

FIGURE 2 | Western blot analysis of *O*-GlcNAcylation levels in HepG2 cells following treatment with compounds **3** and **4**. (A,B) *O*-GlcNAcylation levels were compared with those observed after treatment with Ac_4-5SGlcNAc, used as a positive control for OGT inhibition. The relative intensity (Rel. Int.) of each lane is indicated (*O*-GlcNAc/GAPDH or *O*-GlcNAc/tubulin), compared to the lane vehicle as control. MW standards are indicated in kDa.

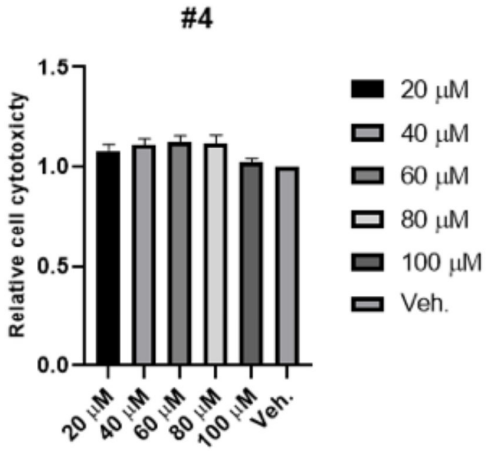

FIGURE 3 | Evaluation of the cytotoxic effects of compound **4** in HepG2 cells. Cells were treated with increasing concentrations (20–100 μM) of compound **4** for 16 h. Cell viability was assessed using the CCK-8 assay. Data were normalized against vehicle (Veh.).

2.3 | Evaluation of the Activity of Compounds 3 and 4 in Cultured Cells

To assess the potential of the imino-*C*-glycosides to inhibit the activity of OGT within a cellular context, we tested only the two most potent OGT inhibitors **3** and **4** of the series in HepG2 cells. With compound **3**, no change in the *O*-GlcNAc profile was observed for this compound neither at 50 μM nor at 100 μM whereas Ac_4-5SGlcNAc dramatically reduced *O*-GlcNAcylation level (Figure 2a). We then assayed the GalNAc derivative **4** and observed a slight dose-dependent decrease in *O*-GlcNAcylation levels (Figure 2b). Therefore, it appears that the inhibitory effect of GlcNAc-1-phosphate mimetics on *O*-GlcNAcylation profiles is more significant with the GalNAc derivative **4** than with its GlcNAc counterpart **3**. We next checked the putative toxic effect of the imino-*C*-glycoside **4** in cultured cells by using the MTS test. No noticeable toxicity was detected for compound **4** (Figure 3).

3 | Conclusion

A small set of imino-*C*-glycosides of α-D-GlcNAc-1-phosphate **3**, **5** and **6** and a D-galacto analog **4** were synthesized and evaluated for inhibition of OGT. The synthetic procedure provides an access to UDP-*C*-*5N*GlcNAc **5.** Our results demonstrated that the connection of iminosugar phosphonate **3** with a uridine motif via a pyrophosphate group results in weak hOGT inhibitors, a surprising result that leads one to consider the nature of the oxocarbenium ion character of the proposed transition state used

by OGT. Interestingly, the α-D-GalNAc-1-phosphate analog **4** proved to be a better inhibitor that seems to bind outside the active site. The nature and identification of this site are intriguing. The pyrophosphate coupling reported herein could therefore be used for the synthesis of analogs of UDP-GalNAc, which could result in potential inhibitors of OGT and GalNAc transferases of therapeutic interest [37].

4 | Experimental Section

Essential Experimental Procedures/Data.

4.1 | General Information

All commercially available reagents were used as supplied without further purification. Petroleum ether (PE) refers to the 40 °C–60 °C boiling fraction. Air- and water-sensitive reactions were performed in "flame" dried glassware under Ar atmosphere. For reactions that require heating, Radleys Heat-On block systems were used. TLC plates (MachereyNagel – Alugram SIL G/UV254) were visualized under 254 nm UV light and/or by dipping the TLC plate into a solution of phosphomolybdic acid in ethanol (3 g/100 mL) followed by heating with a heat gun. Flash chromatography columns were performed using silica gel 60 (15–40 μm) or carried on a Combiflash Rf automated apparatus (Teledyne-Isco) using columns specified in each protocol. When no column is mentioned, the product was purified on standard silica (Macherey–Nagel 60, 14–40 μm). NMR experiments were recorded with a Bruker 400 Avance III Plus spectrometer at 400 and 101 MHz for ^{1}H and ^{13}C, respectively, and with a Bruker Ultrashield 500 Avance NEO spectrometer at 500 and 125 MHz for ^{1}H and ^{13}C nuclei, respectively. Spectra were calibrated using the residual deuterated solvent peak and chemical shifts are expressed in part per million (ppm). NMR multiplicities are reported using the following abbreviations: b = broad, s = singlet, d = doublet, t = triplet, q = quadruplet, m = multiplet. Structural assignments were made with additional information from gCOSY, gHSQC, and gHMBC experiments. HRMS was obtained with a Q-TOF spectrometer from the Mass Spectrometry Service (IC2MP, UMR CNRS 7285-Poitiers University, France). Optical rotations were measured using a Modular Circular Polarimeter MCP100 (Anton Paar).

4.2 | Synthesis

4.2.1 | 2-Acetamido-1,2,5-Trideoxy-1,5-Imino-1-C-Phosphonomethyl-α-D-Glucitol Hydroiodide 3

At 0 °C under argon atmosphere, TMSI (305 μL, 2.14 mmol, 22 eq.) was added dropwise to a solution of iminosugar **1** (38 mg, 97 μmol, 1 eq.) in CH_2Cl_2 (2 mL) and the reaction was allowed to stir at room temperature for 8 h. Then, methanol (4 mL) was added, and the mixture was stirred for another 20 min before being concentrated in vacuo. The crude mixture was dissolved in water (10 mL) and extracted with diethyl ether (8 × 10 mL). The aqueous layer was concentrated with methanol (3 × 10 mL) and passed through a Sephadex G-25 column (eluent: H_2O). The collected fractions were lyophilized to afford compound **3** (32 mg, 75 μmol, 77%) as a colorless amorphous solid. $[\alpha]_D^{20}$ = +45 (c 0.25, CH_3OH); ^{1}H NMR (500 MHz, D_2O): δ (ppm) = 4.13 (ddd, 1H, $J_{2,3}$ = 10.9 Hz, $J_{2,1}$ = 5.4 Hz, $J_{2,P}$ = 2.2 Hz, H-2), 3.97–3.91 (m, 1H, H-1), 3.90 (dd, 1H, $J_{6a,6b}$ = 12.8 Hz, $J_{6a,5}$ = 3.4 Hz, H-6a), 3.85 (dd, 1H, $J_{6b,6a}$ = 12.8 Hz, $J_{6b,5}$ = 5.5 Hz, H-6b), 3.69 (dd, 1H, $J_{3,2}$ = 10.9 Hz, $J_{3,4}$ = 9.0 Hz, H-3), 3.59 (dd, 1H, $J_{4,5}$ = 10.5 Hz, $J_{4,3}$ = 9.0 Hz, H-4), 3.35 (ddd, 1H, $J_{5,4}$ = 10.5 Hz, $J_{5,6b}$ = 5.5 Hz, $J_{5,6a}$ = 3.4 Hz, H-5), 2.03–1.86 (m, 2H, H-1′), 1.99 (s, 3H, CH_3); $^{13}C\{^{1}H\}$ NMR (125 MHz, D_2O): δ (ppm) = 174.4 (CO), 68.9 (C-3), 68.8 (C-4), 57.7 (C-6), 54.5 (C-5), 50.7 (d, $J_{2,P}$ = 13.1 Hz, C-2), 50.5 (d, $J_{1,P}$ = 4.0 Hz, C-1), 21.7 (CH_3), 21.6 (d, $J_{1',P}$ = 129.0 Hz, C-1′); ^{31}P NMR (202 MHz, D_2O): δ (ppm) = 18.6; HRMS (ESI^+) m/z: $[M+H]^+$ calcd. for $C_9H_{20}N_2O_7P$ 299.1003, found: 299.0999.

4.2.2 | Diethyl (((2S, 3S,4R, 5R,6R)-3-Acetamido-4,5-Diacetoxy-6-Acetoxymethyl)piperidin-2-yl)methyl) Phosphonate 3′

Acetic anhydride (10 μL, 0.10 mmol, 3 eq.) was added to a stirred solution of compound **1** (12 mg, 34 μmol, 1 eq.) in dry pyridine (0.3 mL). The solution was stirred at room temperature for 2 h, concentrated and coevaporated with toluene. The crude residue was purified by a flash chromatography column (EtOAc/MeOH 90:10) to afford compound **3′** (11 mg, 23 μmol, 68%) as a colorless oil. $[\alpha]_D^{20}$ = +35 (c 0.125, CH_3OH); ^{1}H NMR (500 MHz, CD_3OD): δ (ppm) = 5.03 (dd, 1H, $J_{3,2}$ = 10.7 Hz, $J_{3,4}$ = 8.7 Hz, H-3), 4.80 (dd, 1H, $J_{4,5}$ = 9.4 Hz, $J_{4,3}$ = 8.7 Hz, H-4), 4.18 (ddd, 1H, $J_{2,3}$ = 10.7 Hz, $J_{2,1}$ = 5.2 Hz, $J_{2,P}$ = 2.7 Hz, H-2), 4.14–4.04 (m, 5H, H-6a, OCH_2CH_3), 4.02 (dd, 1H, $J_{6b,6a}$ = 11.4 Hz, $J_{6b,5}$ = 3.2 Hz, H-6b), 3.55 (tdd, 1H, $J_{1,1'}$ = 11.2 Hz, $J_{1,2}$ = 5.2 Hz, $J_{1,P}$ = 3.2 Hz, H-1), 3.17 (ddd, 1H, $J_{5,4}$ = 9.4 Hz, $J_{5,6a}$ = 5.3 Hz, $J_{5,6b}$ = 3.2 Hz, H-5), 2.26–2.16 (m, 1H, H-1′a), 2.02 (s, 3H, CH_3CO), 2.02–1.92 (m, 1H, H-1′b), 1.97 (s, 3H, CH_3CO), 1.95 (s, 3H, CH_3CO), 1.90 (s, 3H, CH_3CO), 1.28 (td, 6H, $J_{CH3,CH2}$ = 7.1 Hz, $J_{CH3,P}$ = 1.4 Hz, OCH_2CH_3); $^{13}C\{^{1}H\}$ NMR (125 MHz, CD_3OD): δ (ppm) = 173.3, 172.5, 172.0, 171.6 (CO), 72.6 (C-4), 72.2 (C-3), 62.8 (C-6), 63.6 (d, $J_{CH2,P}$ = 6.6 Hz, OCH_2CH_3), 63.4 (d, $J_{CH2,P}$ = 6.5 Hz, OCH_2CH_3), 54.0 (d, $J_{2,P}$ = 14.8 Hz, C-2), 52.2 (C-5), 50.7 (d, $J_{1,P}$ = 4.4 Hz, C-1), 23.8 (d, $J_{1',P}$ = 143.8 Hz, C-1′), 22.5, 20.7, 20.7 (CH_3CO), 16.7 (d, $J_{CH3,P}$ = 6.1 Hz, OCH_2CH_3). ^{31}P NMR (202 MHz, CD_3OD): δ (ppm) = 30.9; HRMS (ESI^+) m/z: $[M+Na]^+$ calcd. for $C_{19}H_{33}N_2NaO_{10}P$ 503.1765, found: 503.1753.

4.2.3 | 2-Acetamido-1,2,5-Trideoxy-1,5-Imino-1-C-Phosphonomethyl-α-D-Galactitol Hydroiodide 4

At 0 °C under argon atmosphere, TMSI (80 μL, 0.56 mmol, 22 eq.) was added dropwise into a solution of iminosugar **2** (10 mg, 26 μmol, 1 eq.) in CH_2Cl_2 (1 mL) and the reaction was allowed to stir at room temperature for 8 h. Then, methanol (2 mL) was added and the mixture was stirred for another 20 min before being concentrated in vacuo. The crude mixture was dissolved in water (5 mL) and extracted with diethyl ether (8 × 5 mL). The aqueous layer was concentrated with methanol (3 × 5 mL) and passed through an Sephadex G-25 column (eluent: H_2O). The collected fractions were lyophilized to afford compound **4** (8.5 mg, 20 μmol, 77%) as a colorless amorphous solid. $[\alpha]_D^{20}$ = +43 (c 0.125, H_2O); ^{1}H NMR (500 MHz, D_2O): δ (ppm) = 4.38 (ddd, 1H, $J_{2,3}$ = 11.3 Hz, $J_{2,1}$ = 5.5 Hz, $J_{2,P}$ = 1.7 Hz, H-2), 4.06 (bs, 1H, H-4), 3.93 (ddd, 1H, $J_{1,1'a}$ = 14.1 Hz, $J_{1,1'b}$ = 10.6 Hz, $J_{1,2}$ = 5.5 Hz, H-1), 3.83–3.72 (m, 2H, H-3 and H-6a), 3.85 (dd, 1H, $J_{6b,6a}$ = 12.1 Hz, $J_{6b,5}$ = 9.0 Hz, H-6b), 3.53 (dd, 1H, $J_{5,6b}$ = 9.0 Hz, $J_{5,6a}$ = 4.2 Hz, H-5), 1.99 (s, 3H, CH_3); $^{13}C\{^{1}H\}$ NMR (125 MHz, D_2O): δ (ppm) = 174.7 (CO), 65.9 (C-3), 65.8 (C-4), 58.9 (C-6), 54.3 (C-5), 50.7 (C-1), 47.2

(d, $J_{2,P}$ = 13.0 Hz, C-2), 21.7 (CH_3), 21.6 (d, $J_{1',P}$ = 128.8 Hz, C-1′); ^{31}P NMR (202 MHz, D_2O): δ (ppm) = 19.1; HRMS (ESI^+) m/z: $[M+H]^+$ calcd. for $C_9H_{20}N_2O_7P$ 299.1003, found: 299.1012.

4.2.4 | *Uridine-5′-Phosphorimidazolide*

Uridine monophosphate (UMP) free acid was basified in a mixture containing EtOH:H_2O:NEt_3 under vigorous stirring for 16 h. Then, the solution was lyophilized to give the triethylammonium salt as a white solid. To a solution of UMP triethylammonium salt (468 mg, 0.813 mmol, 1.0 equiv.) were added 2,2′-dipyridyl disulfide (538 mg, 2.44 mmol, 3.0 equiv.) and imidazole (554 mg, 8.13 mmol, 10 equiv.) in anhydrous DMF (8 mL). After 10 min, were added triethylamine (0.45 mL, 3.25 mmol, 4 equiv.) and triphenylphosphine (640 mg, 2.44 mmol, 3.0 equiv.) at room temperature under argon. The reaction was stirred for 16 h. The desired product was precipitated from the reaction mixture by an anhydrous solution of $NaClO_4$ (1.6 g) in dry acetone (130 mL). The suspension was cooled at 0 °C under argon. The precipitate was filtered, washed with cold dry acetone, and dried in vacuo over P_4O_{10}, to yield uridine-5′-phosphorimidazolide (306 mg, 95%) as a white solid. ^{1}H-NMR (400 MHz, D_2O): δ 7.86 (br, 1H, H-im), 7.62 (d, J_{6u-5u} = 8.2 Hz, 1H, H-6u), 7.23 (br, 1H, H-im), 7.06 (br, 1H, 1H-im), 5.83 (d, J_{1r-2r} = 4.8 Hz, 1H, H-1r), 5.81 (d, J_{5u-6u} = 8.2 Hz, 1H, H-5u), 4.23 (d, J_{2r-1r} = 4.8 Hz, 1H, H-2r), 4.12–4.07 (m, 3H, H-3r, H-4r, H-5r_b), 3.98–3.94 (m, 1H, H-5r_a). ^{13}C-NMR (100 MHz, D_2O): δ 166.6 −141.2 (4x C-u), 139.9 (C-im), 129.3 (C-im), 120.1 (C-im), 102.5 (C-5u), 88.9 (C-1r), 82.5 (C-4r), 73.6 (C-2r), 69.3 (C-3r), 65.0 (C-5r).^{31}P-NMR (200 MHz, D_2O): δ −7.51 (s, 1P). HRMS (ESI^-) m/z: $[M-H]^-$ calc. for $C_{12}H_{14}N_4O_8P$ 373.0518, found: 373.0555.

4.2.5 | *Bis(triethylammonium) 2-Acetamido-1,2,5-Trideoxy-1,5-Imino-1-C-Phosphonomethyl-α-D-Glucitol-Uridin-5′-yl Phosphate 5*

The iminosugar **3** (23 mg, 0.037 mmol, 1 equiv.) and $MgCl_2$ (7 mg, 0.074 mmol, 2 equiv.) were stirred in anhydrous DMF (0.5 mL) for approximately 10 min. To this mixture was then added a solution of uridine-5′-phosphorimidazolide sodium salt (24 mg, 0.055 mmol, 1.5 equiv.) in anhydrous DMF (0.5 mL) under argon. This reaction was stirred for 20 h at room temperature. To the mixture was added water (HPLC grade) and the solution was lyophilized to give the crude product. The latter was purified by reverse phase HPLC (Zorbax SB-C18, mobile phase: $AcO^-Et_3NH^+$, pH = 6.8, flow rate 15 mL min^{-1}, ret.time 20 min) to afford pure nucleotide iminosugar **5** (3.5 mg, 10%) as white powder. ^{1}H-NMR (400 MHz, D_2O): δ 7.85 (d, J_{6u-5u} = 8.2 Hz, 1H, H-6u), 5.93 (br, 1H, H-1r), 5.87 (d, J_{5u-6u} = 8.2 Hz, 1H, H-5u), 4.30 (m, 2H, H-2r, H-3r), 4.20 (m, 1H, H-2), 4.14 (m, 2H, H-4r, H-5r), 3.87 (m, 2H, H-6), 3.52–3.45 (m, 3H, H-1, H-4, H-5), 2.07 (m, CH_2), 1.98 (s, 3H, CH_3). ^{13}C-NMR (100 MHz, D_2O): δ 181.52–174.34 (C=O), 141.2 (C-6u), 102.74 (C-5u), 88.48 (C-1r), 73.74–62.26 (C-r, C-3, C-4, C-6), 54.04 (C-5),23.21 (CH2), 22.01 (CH3).^{31}P-NMR (200 MHz, D_2O): δ 15.75 (d, J = 26.6 Hz, 1P), −10.67 (d, J = 26.6 Hz, 1P). HRMS (ESI^-) m/z: $[M-H]^-$ calc. for $C_{18}H_{29}N_4O_{15}P_2$ 603.1102, found: 603.1110.

4.2.6 | *2-Acetamido-N-Benzyl-3,4,6-Tri-O-Benzyl-1,2,5-Trideoxy-1,5-Imino-1-C-(azidomethyl)-α-D-Glucitol 8*

To a stirred solution of azide **7** (55 mg, 0.10 mmol, 1 eq.) in a 1:1 v/v mixture of EtOAc/H_2O (2 mL) were added $KHCO_3$ (207 mg, 2.07 mmol, 20 eq.) and BnBr (74 µL, 0.62 mmol, 6 eq.). The mixture was stirred at 80 °C. After 24 h, the mixture was quenched with H_2O then extracted thrice with Et_2O. Combined organic layers were dried over $MgSO_4$ and concentrated under reduced pressure. Purification by silica gel chromatography (toluene/EtOAc 65:35) afforded *N*-benzyl iminosugar **8** (55 mg, 89 µmol, 85%) as colorless oil. R_f = 0.55 (toluene/EtOAc 65:35); $[\alpha]_D^{20}$ = - 69 (c 0.25, $CHCl_3$); ^{1}H NMR (400 MHz, $CDCl_3$): δ (ppm) 7.38–7.19 (m, 20H, H_{Ar}), 6.64 (d, 1H, $J_{NH,2}$ = 8.8 Hz, NH), 4.64, 4.56 (AB, 2H, J_{AB} = 11.8 Hz, CH_2Ph), 4.42, 4.39 (AB, 2H, J_{AB} = 11.6 Hz, CH_2Ph), 4.45, 4.35 (AB, 2H, J_{AB} = 11.1 Hz, CH_2Ph), 4.32–4.27 (m, 1H, H-2), 4.04 (d, 1H, ^2J = 14.6 Hz, NCHPh), 3.90 (d, 1H, ^2J = 14.6 Hz, NCHPh), 3.88–3.77 (m, 3H, H-1′, H-4), 3.67 (dd, 1H, $J_{3,2} = J_{3,4}$ = 3.1 Hz, H-3), 3.45–3.30 (m, 4H, H-1, H-5, H-6), 1.79 (s, 3H, CH_3); ^{13}C{^{1}H} NMR (101 MHz, $CDCl_3$): δ (ppm) 169.8 (CO), 140.8, 138.4, 138.0, 138.0 (Cq_{Ar}), 128.6, 128.6, 128.5, 128.4, 128.2, 128.0, 128.0, 127.7, 127.7, 127.6, 127.1 (CH_{Ar}), 76.3 (C-3), 75.2 (C-4), 73.3, 72.3, 71.8 (CH_2Ph), 66.4 (C-1′), 58.8 (C-5), 53.6 (NCH_2Ph), 53.5 (C-1), 52.0 (C-6), 48.9 (C-2), 23.5 (CH_3); HRMS (ESI) m/z: $[M+K]^+$ calcd for $C_{37}H_{41}KN_5O_4$ 658.2790, found: 658.2786.

4.2.7 | *5′-(2-Ethoxy-3,4-Dioxo-1-Cyclobuten-1-yl)amino-5′-Deoxy-2′, 3′-O-Isopropylidene Uridine 10*

5′-amino-uridine **9** (67 mg, 0.24 mmol, 1 eq.) was dissolved in ethanol (1 mL) then diisopropylethylamine (21 µL, 0.118 mmol, 0.5 eq.) and 3,4-diethoxy-cyclobutene-1,2-dione (42 µM, 0.28 mmol, 1.2 eq.) were added. The mixture was stirred for 2 h at room temperature. The reaction mixture was then concentrated under reduced pressure. Purification by column chromatography ($CHCl_3$/MeOH 95:5) afforded compound **10** (80 mg, 0.20 mmol, 83%) as a white foam. R_f = 0.38 (CH_2Cl_2/EtOH 95:5); $[\alpha]_D^{20}$ = - 39 (c 1.0, $CHCl_3$); ^{1}H NMR (500 MHz, acetone-d6): δ (ppm) = 10.28 (br s, 1H, NH-uridine), 7.81 (br s, 1H, NH squaramide), 7.68–7.64 (m, 1H, H-6u), 5.73 (d, 1H, $J_{1'',2''}$ = 1.7 Hz, H-1″), 5.65 (d, 1H, $J_{5u,\ 6u}$ = 7.9 Hz, H-5u), 5.17 (dd, 1H, $J_{2'',\ 3''}$ = 6.2 Hz, $J_{2'',1''}$ = 1.7 Hz, H-2″), 4.90 (dd, 1H, $J_{3'',2''}$ = 6.2 Hz, $J_{3'',4''}$ = 4.5 Hz, H-3″), 4.73–4.65 (m, 2H, OC***H*****$_2$**CH_3), 4.24 (app q, H-4″), 4.05–3.90 (m, 1H, H-5″a), 3.79 (br s, 1H, H-5″b), 1.50 (s, 3H, CH_3), 1.44–1.37 (m, 3H, OCH_2C***H*****$_3$**), 1.32 (s, 3H, CH_3); ^{13}C{^{1}H} NMR (125 MHz, acetone-d6): δ (ppm) 189.9, 189.7, 184.0, 183.9 (CO-cyclobutene), 178.4, 178.0, 174.3, 173.9 (Cq_{Ar}-cyclobutene), 163.8, 151.33 (CO-uridine), 144.5, 144.4 (C-6u), 114.7 (***C***$(CH_3)_2$), 102.8 (C-5u), 95.3 (C-1″), 87.6, 87.4 (C-4″), 85.1 (C-2″), 82.4, 82.4 (C-3″), 69.8 (O***C***H_2CH_3), 46.9, 46.6 (C-5″), 27.4 (CH_3), 25.4 (CH_3), 16.1, 16.0 (OCH_2***C***H_3); HRMS (ESI) m/z: $[M+K]^+$ calcd for $C_{18}H_{21}KN_3O_8$ 446.0960, found: 446.0950.

4.2.8 | *2-Acetamido-1,5-Benzylimino-3,4,6-Tri-O-Benzyl-1,2,5-Trideoxy-1-C-((2-(5′-Deoxy-2′, 3′-O-Isopropylidene-Uridin-5′-yl) amino-3,4-Dioxo-1-Cyclobuten-1-yl)aminomethyl-α-D-Glucitol 11*

A stirred solution of compound **8** (15 mg, 24 µmol, 1 eq.) in methanol (1 mL) was flushed 3 times with argon and 10% wt Pd/C (2 mg) was added. The mixture was flushed 4 times with H_2 and stirred for 1 h under H_2 atmosphere. The mixture was then filtered over a pad of Celite and the filtrate was concentrated under reduced pressure. To a solution of crude amine **8′** and compound **10** (15 mg, 36 µmol, 1.5 eq.) in ethanol (0.5 mL) was added DIPEA (6 µL, 36 µmol, 1.5 eq.) The mixture

was stirred for 2 h at room temperature then was concentrated under reduced pressure. Purification by silica gel chromatography (EtOAc/MeOH 100:1) afforded compound **11** (18 mg, 19 µmol, 78%) as a colorless oil. R_f = 0.3 (CH_2Cl_2/MeOH 20:1); $[\alpha]_D^{20}$ = −14 (c 1.0, $CHCl_3$); ^{1}H NMR (400 MHz, $CDCl_3$): δ (ppm) 7.60 (d, 1H, $J_{NH,2}$ = 9.3 Hz, NH), 7.61–7.06 (m, 21H, H_{Ar} and H-6u), 7.07 (d, 1H, J = 8.7 Hz, NH squaramide), 6.54 (dd, 1H, $J_{NH,1'a}$ = 8.2 Hz, $J_{NH,1'b}$ = 4.6 Hz, NH squaramide), 5.76 (dd, 1H, $J_{5u,6u}$ = 8.0 Hz, $J_{5u,3u}$ = 2.2 Hz, H-5u), 5.23 (d, 1H, $J_{1'',2''}$ = 2.6 Hz, H-1″), 5.19 (d, 1H, $J_{2'',3''}$ = 6.9 Hz, $J_{2'',1''}$ = 2.6 Hz, H-2″), 4.85 (d, 1H, $J_{3'',2''}$ = 6.9 Hz, $J_{3'',4''}$ = 4.3 Hz, H-3″), 4.57 (d, 1H, ^{2}J = 11.1 Hz, CHPh), 4.53, 4.45 (AB, 2H, J_{AB} = 11.9 Hz, CH_2Ph), 4.47, 4.41 (AB, 2H, J_{AB} = 11.9 Hz, CH_2Ph), 4.38 (d, 1H, ^{2}J = 11.1 Hz, CHPh), 4.38–4.28 (m, 3H, H-1′a, H-4″, H-5″a), 4.15 (d, 1H, ^{2}J = 15.1 Hz, NCHPh), 4.08 (br d, 1H, $J_{2,NH}$ = 9.3 Hz, H-2), 3.94–3.83 (m, 4H, H-4, H-6, NCHPh), 3.78 (dd, 1H, $J_{5''b,5''a}$ = 14.3 Hz, $J_{5''b,4''}$ = 3.1 Hz, H-5″b), 3.69 (br s, 1H, H-3), 3.46–3.38 (m, 2H, H-5, H-1), 2.47 (ddd, 1H, $J_{1'b,1'a}$ = 13.3 Hz, $J_{1'b,1}$ = 13.3 Hz, $J_{1'b,NH}$ = 4.6 Hz, H-1′b), 1.91 (s, 3H, CH_3CO), 1.54 (s, 3H, CH_3), 1.29 (s, 3H, CH_3); ^{13}C{^{1}H} NMR (100 MHz, $CDCl_3$): δ (ppm) 183.8, 183.5 (CO-cyclobutene), 171.8 (CH_3CO), 168.4, 167.6 (Cq_{Ar}-cyclobutene), 162.9, 152.8 (CO-uridine), 143.8 (C-6u), 141.7, 138.4, 137.7, 137.5 (Cq_{Ar}), 128.8, 128.6, 128.5, 128.3, 128.3, 128.1, 127.8, 127.8, 127.7, 127.7, 126.9 (CH_{Ar}), 115.2 (Cq-Me_2), 104.0 (C-5u), 99.4 (C-1″), 86.0 (C-4″), 83.5 (C-2″), 80.2 (C-3″), 75.4 (C-3), 74.5 (C-4), 73.4, 72.5, 71.6 (CH_2Ph), 65.5 (C-6), 61.2 (C-5), 55.7 (C-1), 54.6 (NCH_2Ph), 47.5 (C-2), 45.1 (C-5″), 43.5 (C-1′), 27.1 (CH_3), 25.1 (CH_3), 23.3 (CH_3CO); HRMS (ESI) m/z: $[M+Na]^+$ calcd for $C_{53}H_{58}N_6NaO_{11}$ 977.4056, found: 977.4096.

4.2.9 | 2-Acetamido-1,5-Benzylimino-3,4,6-Tri-O-Benzyl-1,2,5-Trideoxy-1-C-((2-(5′-Deoxy-Uridin-5′-yl)amino-3,4-Dioxo-1-Cyclobuten-1-yl)aminomethyl-α-D-Glucitol 6

To a solution of iminoglycoconjugate **11** (10 mg, 10 µmol, 1 eq.) in anhydrous THF (0.15 mL) was added dropwise a 1:1 v/v mixture of TFA/H_2O (0.3 mL). The mixture was stirred at room temperature for 2 h then the mixture concentrated under reduced pressure with repeated co-evaporation with toluene (x2). Purification by flash chromatography (CH_2Cl_2/MeOH 17:1) afforded compound **6** (8 mg, 8 µmol, 84%) as an amorphous solid. R_f = 0.25 (CH_2Cl_2/MeOH 50:3); $[\alpha]_D^{20}$ = +42 (c 0.05, MeOH); ^{1}H NMR (500 MHz, CD_3OD): δ (ppm) 7.67 (bs, 1H, NH), 7.34–7.18 (m, 21H, H_{Ar} and H-6u), 7.07 (d, 1H, $J_{6u,5u}$ = 8.0 Hz, H-6u), 6.54 (d, 1H, $J_{5u,6u}$ = 8.0 Hz, H-5u), 5.23 (d, 1H, $J_{1'',2''}$ = 2.6 Hz, H-1″), 5.19 (d, 1H, $J_{2'',3''}$ = 6.8 Hz, $J_{2'',1''}$ = 2.6 Hz, H-2″), 4.85 (d, 1H, $J_{3'',2''}$ = 6.8 Hz, $J_{3'',4''}$ = 4.3 Hz, H-3″), 4.57 (d, 1H, ^{2}J = 11.1 Hz, CHPh), 4.53 (d, 1H, ^{2}J = 12.1 Hz, CHPh), 4.47, 4.45 (AB, 2H, J_{AB} = 11.8 Hz, CH_2Ph), 4.42–4.29 (m, 3H, H-4″, H-5″a, H-6a), 4.15 (d, 1H, ^{2}J = 15.1 Hz, NCHPh), 4.09–4.06 (m, 1H, H-2), 3.94–3.84 (m, 4H, H-4, NCHPh, H-1′), 3.78 (dd, 1H, $J_{6b,6a}$ = 14.3 Hz, $J_{6b,5}$ = 3.1 Hz, H-6b), 3.69 (bs, 1H, H-3), 3.45–3.39 (m, 2H, H-5, H-1), 2.51–2.44 (m, 1H, H-5″b), 1.91 (s, 3H, CH_3); ^{13}C{^{1}H} NMR (101 MHz, CD_3OD): δ (ppm) 183.8, 183.8 (C=O-cyclobutene), 173.3 (C=O), 169.3, 169.3 (Cq_{Ar}-cyclobutene), 166.0, 152.3 (C=O-uridine), 143.6 (C-6u), 139.9, 139.7, 139.1 (Cq_{Ar}), 129.5, 129.5, 129.4, 129.3, 129.0, 128.9, 128.8, 129.7, 128.6 (CH_{Ar}), 103.1 (C-5u), 93.1 (C-1″), 84.4 (C-4″), 83.5 (C-2″), 80.2 (C-3″), 75.4 (C-3), 74.5 (C-4), 73.4, 72.5, 71.6 (CH_2Ph), 65.5 (C-1′), 61.2 (C-5), 55.7 (C-1), 54.6 (NCH_2Ph), 47.5 (C-2), 45.1 (C-5″), 41.5 (C-6), 22.9 (CH_3); HRMS (ESI) m/z: $[M+H]^+$ calcd for $C_{50}H_{55}N_6O_{11}$ 915.3923, found: 915.395.

4.3 | Enzymatic Synthesis

*Sp*GalU encoding gene [38] was synthesized (Eurofins Genomics) and cloned into pET28a(+) expression vector (Merck Biosciences). The construct was then transformed in BL21(DE3) *E. coli* cells. Induction of *Sp*GalU encoding gene was done at 22 °C using 0.2 mM IPTG, cells were harvested, lyzed, and recombinant *Sp*GalU was purified using NiNTA column. *E. coli* pyrophosphorylase *Ec*PPase was obtained as reported previously [39]. The deprotected iminosugar **3** (15 mg, 0.035 mmol, 1 equiv.) was added to the reaction mixture (35 mL, 50 mM HEPES pH 7.5), containing UTP (38.9 mg, 0.070 mmol, 2 equiv.), Potassium Phosphoenolpyruvate (14.58 mg, 0.070 mmol, 2 equiv.), 10 mM $MgCl_2$, 10 mM KCl, 1U/mL Pyruvate Kinase from rabbit muscle (Sigma–Aldrich), 0.2 mg/mL *Ec*PPase and 1 mg/mL *Sp*GalU. The reaction was heated and stirred at 30 °C. HPLC analysis of reaction using reported conditions [39] indicated that the conversion rate of the enzymatic reaction reached a plateau at 3.6% after 24 h of reaction. No further evolution could be seen, even by adding additional enzymes.

The reaction was evaporated, lyophilized, and resuspended in water before anionic exchange purification on DEAE-sepharose column (Cytiva) using sodium carbonate step gradient for elution [39]. Size exclusion chromatography on P-2 gel column (Bio-Rad) was then performed using water as eluent. **5** coeluted with UMP, the latter was specifically hydrolyzed into uridine and phosphate using alkaline phosphate (FastAP, Thermoscientific) for 1 h at 37 °C. **5** was finally purified by a second P-2 gel column (0.5 mg, 0.007 mM, 2 % yield). HRMS, ^{1}H- and ^{31}P NMR analyses of **5** obtained by enzymatic synthesis were in accordance with those presented above.

4.4 | Evaluation of the Activity of Compounds 3 and 4 in Cultured Cells

The human hepatocarcinoma derived-cell line HepG2 (provided by the ATCC) was cultured in Dulbecco's Modified Eagle's Medium (DMEM, Lonza) supplemented with 25 mM glucose and 10% (v/v) fetal calf serum (Dominique Dutscher) and 2 mM L-glutamine and maintained at 37 °C in a 5% (v/v) CO_2-enriched, humidified atmosphere. Cells were seeded in 12-well plate at a density of 80.000 cells per well and treated with compound **3** at 50 or 100 µM for 16 h, or with compound **4** at concentrations ranging from 20 to 100 µM for 16 h. Ac_4-5SGlcNAc was used at 50 µM as a positive control, and the vehicle (water) was considered as a negative control. Cells were lyzed in Laemmli buffer (200 µL per well). After homogenization by using a vortex shaker, cell extracts were centrifuged at 20.000 x *g* 10 min at 4°C. Supernatants were transferred in clean tubes and boiled for 5 min. Proteins were resolved by 7.5% SDS-PAGE in electrophoresis buffer (25 mM Tris-HCl, 192 mM glycine, 0.1% (m/v) SDS, pH 8.8) and transferred onto nitrocellulose membranes (HybondTM-C EXTRA, GE Healthcare) in transfer buffer (25 mM Tris-HCl, 192 mM glycine, 20% (v/v) methanol, pH 8,8). Membranes were stained with Ponceau red (5% (v/v) acetic acid and 0,1% (w/v) Ponceau red) to assess equal loading. Membranes were destained with TBS (Tris-Buffered Saline) – Tween20 (20 mM Tris-HCl, 150 mM NaCl, 0,05% (v/v) Tween20 (Sigma–Aldrich), pH 7,5) (TBS-T), subsequently blocked in 5% (w/v) nonfat dry milk or BSA in TBS-T, and

probed overnight at 4 °C with primary antibodies: mouse monoclonal anti-*O*-GlcNAc (RL2, Thermo Scientific), at a dilution of 1:2.000; mouse monoclonal anti-GAPDH (71548, Covalab), at a dilution of 1:4.000; and rabbit polyclonal anti-β-tubulin (H-235: sc-9104, Santa Cruz Biotechnology) at a dilution of 1:1.000. After three TBS-T washes, membranes were incubated with the appropriate horseradish peroxidase-conjugated secondary antibody, anti-mouse or anti-rabbit IgG-HRP linked (GE Healthcare), at a dilution of 1:10.000 for 1 h at room temperature. After three TBS-T washes, blots were developed using enhanced chemiluminescence (West Pico Plus, ThermoScientific). The images were acquired using a CCD camera (Fusion Solo, Vilbert Lourmat).

4.5 | Cell Viability Assay

HepG2 cells were seeded in 96-well plates and treated with compound **4** at various concentrations (20–100 μM) for 16 h. The cytotoxic effect of compound **4** was evaluated by measuring cell viability using the CCK-8 assay (MedChemExpress), according to the manufacturer's instructions.

Acknowledgments

Y.B. acknowledges financial support from the European Union (ERDF) and "Région Nouvelle Aquitaine". T.T.V. thanks Fondation pour la Recherche Médicale for a PhD grant. We thank R. Meek (University of Southampton) for crystallization attempts of the OGT-compound **4** complex. AP and PL thank SALSA platform for HRMS and NMR analysis, as well as Project ESTIM-ICOA (CPER/FEDER-FSE+ 2021-2027-00022860), Labex IRON (ANR-11-LABX-0018-01), and Labex SYNORG (ANR-11-LABX-0029).

Funding

This study was supported by Fondation pour la Recherche Médicale; Labex Iron (ANR-11-LABX-0018-01); Labex SynOrg (ANR-11-LABX-0029).

Conflicts of Interest

The authors declare no conflicts of interest.

Data Availability Statement

The data that support the findings of this study are available in the Supporting Information of this article.

References

1. L. L. Lairson, B. Henrissat, G. J. Davies, and S. G. Withers, "Glycosyltransferases: Structures, Functions, and Mechanisms," *Annual Review of Biochemistry* 77 (2008): 521–555.

2. C. R. Torres and G. W. Hart, "Topography and Polypeptide Distribution of Terminal N-Acetylglucosamine Residues on the Surfaces of Intact Lymphocytes. Evidence for O-Linked GlcNAc.," *The Journal of Biological Chemistry* 259 (1984): 3308–3317.

3. G. W. Hart, M. P. Housley, and C. Slawson, "Cycling of O-Linked β-N-Acetylglucosamine on Nucleocytoplasmic Proteins," *Nature* 446 (2007): 1017–1022.

4. E. Wulff-Fuentes, R. R. Berendt, L. Massman, et al., "The Human O-GlcNAcome Database and Meta-Analysis," *Scientific Data* 8 (2021): 25.

5. S. A. Yuzwa, M. S. Macauley, J. E. Heinonen, et al., "A Potent Mechanism-Inspired O-GlcNAcase Inhibitor that Blocks Phosphorylation of Tau In Vivo," *Nature Chemical Biology* 4 (2008): 483–490.

6. S. A. Yuzwa and D. J. Vocadlo, "O-GlcNAc and Neurodegeneration: Biochemical Mechanisms and Potential Roles in Alzheimer's Disease and beyond," *Chemical Society Reviews* 43 (2014): 6839–6858.

7. M. G. Alteen, R. W. Meek, S. Kolappan, et al., "Phage Display Uncovers a Sequence Motif that Drives Polypeptide Binding to a Conserved Regulatory Exosite of O-GlcNAc Transferase," *Proceedings of the National Academy of Sciences* 120 (2023): e2303690120.

8. M. B. Lazarus, Y. Nam, J. Jiang, P. Sliz, and S. Walker, "Structure of Human O-GlcNAc Transferase and Its Complex with a Peptide Substrate," *Nature* 469 (2011): 564–567.

9. S. G. Withers and G. J. Davies, "The Case of the Missing Base," *Nature Chemical Biology* 8 (2012): 952–953.

10. M. B. Lazarus, J. Jiang, T. M. Gloster, et al., "Structural Snapshots of the Reaction Coordinate for O-GlcNAc Transferase," *Nature Chemical Biology* 8 (2012): 966–968.

11. R. Trapannone, K. Rafie, and D. M. F. Van Aalten, "O-GlcNAc Transferase Inhibitors: Current Tools and Future Challenges," *Biochemical Society Transactions* 44 (2016): 88–93.

12. R. F. Ortiz-Meoz, J. Jiang, M. B. Lazarus, et al., "A Small Molecule That Inhibits OGT Activity in Cells," *ACS Chemical Biology* 10 (2015): 1392–1397.

13. F. A. Hammel, N. C. Payne, V. M. Marando, R. Mazitschek, and S. Walker, "Identification of a Polypeptide Inhibitor of O-GlcNAc Transferase with Picomolar Affinity," *Journal of the American Chemical Society* 146 (2024): 26320–26330.

14. T. M. Gloster, W. F. Zandberg, J. E. Heinonen, D. L. Shen, L. Deng, and D. J. Vocadlo, "Hijacking a Biosynthetic Pathway Yields a Glycosyltransferase Inhibitor Within Cells," *Nature Chemical Biology* 7 (2011): 174–181.

15. T.-W. Liu, W. F. Zandberg, T. M. Gloster, et al., "Metabolic Inhibitors of O-GlcNAc Transferase That Act In Vivo Implicate Decreased O-GlcNAc Levels in Leptin-Mediated Nutrient Sensing," *Angewandte Chemie International Edition* 57 (2018): 7644–7648.

16. P. Ryan, Y. Shi, M. Von Itzstein, and S. Rudrawar, "Novel Bisubstrate Uridine-Peptide Analogues Bearing a Pyrophosphate Bioisostere as Inhibitors of Human O-GlcNAc Transferase," *Bioorganic Chemistry* 110 (2021): 104738.

17. V. S. Borodkin, M. Schimpl, M. Gundogdu, et al., "Bisubstrate UDP–peptide Conjugates as Human O-GlcNAc Transferase Inhibitors," *The Biochemical Journal* 457 (2014): 497–502.

18. S. Wang, D. L. Shen, D. Lafont, et al., "Design of Glycosyltransferase Inhibitors Targeting Human *O* -GlcNAc Transferase (OGT)," *MedChemComm* 5 (2014): 1172–1178.

19. A. Franconetti, A. Ardá, J. L. Asensio, Y. Blériot, S. Thibaudeau, and J. Jiménez-Barbero, "Glycosyl Oxocarbenium Ions: Structure, Conformation, Reactivity, and Interactions," *Accounts of Chemical Research* 54 (2021): 2552–2564.

20. G. Horne and F. X. Wilson, "Therapeutic Applications of Iminosugars: Current Perspectives and Future Opportunities," in Progress in Medicinal Chemistry (Elsevier, 2011), 135–176.

21. I. Conforti and A. Marra, "Iminosugars as Glycosyltransferase Inhibitors," *Organic & Biomolecular Chemistry* 19 (2021): 5439–5475.

22. J. Hajduch, G. Nam, E. J. Kim, R. Fröhlich, J. A. Hanover, and K. L. Kirk, "A Convenient Synthesis of the C-1-Phosphonate Analogue of UDP-GlcNAc and Its Evaluation as an Inhibitor of O-Linked GlcNAc Transferase (OGT)," *Carbohydrate Research* 343 (2008): 189–195.

23. H. C. Dorfmueller, V. S. Borodkin, D. E. Blair, S. Pathak, I. Navratilova, and D. M. van Aalten, "Substrate and Product Analogues as Human O-GlcNAc Transferase Inhibitors," *Amino Acids* 40 (2011): 781–792.

24. M. L. Mitchell, L. V. Lee, and C.-H. Wong, "Synthesis and Evaluation of Six-Membered GDP-Iminocyclitol," *Tetrahedron Letters* 43 (2002): 5691–5693.

25. C.-H. Hsu, M. Schelwies, S. Enck, et al., "Iminosugar C-Glycoside Analogues of α-D-GlcNAc-1-Phosphate: Synthesis and Bacterial Transglycosylase Inhibition," *The Journal of Organic Chemistry* 79 (2014): 8629–8637.

26. M. Schuster and S. Blechert, "Inhibition of Fucosyltransferase V by a GDP–Azasugar," *Bioorganic & Medicinal Chemistry Letters* 11 (2001): 1809–1811.

27. V. Wittmann and C.-H. Wong, "1 *H* -Tetrazole as Catalyst in Phosphomorpholidate Coupling Reactions: Efficient Synthesis of GDP-Fucose, GDP-Mannose, and UDP-Galactose," *The Journal of Organic Chemistry* 62 (1997): 2144–2147.

28. G. K. Wagner, T. Pesnot, and R. A. Field, "A Survey of Chemical Methods for Sugar-Nucleotide Synthesis," *Natural Product Reports* 26 (2009): 1172–1194.

29. T. V. Tran, J. Désiré, N. Auberger, and Y. Blériot, "Stereoselective Synthesis of 1- *C* -Diethylphosphonomethyl and -Difluoromethyl Iminosugars from Sugar Lactams," *The Journal of Organic Chemistry* 87 (2022): 7581–7585.

30. P. Dabrowski-Tumanski, J. Kowalska, and J. Jemielity, "Efficient and Rapid Synthesis of Nucleoside Diphosphate Sugars from Nucleoside Phosphorimidazolides,"*European Journal of Organic Chemistry* 2013 (2013): 2147–2154.

31. C. J.-M. Frédéric, A. Tikad, J. Fu, et al., "Synthesis of Unprecedented Sulfonylated Phosphono-exo-Glycals Designed as Inhibitors of the Three Mycobacterial Galactofuranose Processing Enzymes," *Chemistry – A European Journal* 22 (2016): 15913–15920.

32. T. Li, A. Tikad, H. Fu, et al., "A General Strategy to Synthesize ADP-7-Azido-Heptose and ADP-Azido-Mannoses and Their Heptosyltransferase Binding Properties," *Organic Letters* 23 (2021): 1638–1642.

33. N.-S. Li, J. Lu, and J. A. Piccirilli, "Efficient Synthesis of Methyl 3,5-Di- *O* -Benzyl-α- d -Ribofuranoside and Application to the Synthesis of 2′- *C* -β-Alkoxymethyluridines," *Organic Letters* 9 (2007): 3009–3012.

34. V. Liautard, V. Desvergnes, K. Itoh, H.-w. Liu, and O. R. Martin, "Convergent and Stereoselective Synthesis of Iminosugar-Containing Gal *f* and UDP-Gal *f* Mimicks: Evaluation as Inhibitors of UDP-Gal Mutase," *The Journal of Organic Chemistry* 73 (2008): 3103–3115.

35. M. Ghirardello, D. Perrone, N. Chinaglia, et al., "UDP-GlcNAc Analogues as Inhibitors of *O* -GlcNAc Transferase (OGT): Spectroscopic, Computational, and Biological Studies," *Chemistry – A European Journal* 24 (2018): 7264–7272.

36. M. G. Alteen, H. Peacock, R. W. Meek, et al., "Potent De Novo Macrocyclic Peptides That Inhibit O-GlcNAc Transferase through an Allosteric Mechanism," *Angewandte Chemie International Edition* 62 (2023): e202215671.

37. I. Compañón, C. J. Ballard, E. Lira-Navarrete, et al., "Rational Design of Dual-Domain Binding Inhibitors for *N* -Acetylgalactosamine Transferase 2 with Improved Selectivity over the T1 and T3 Isoforms," *JACS Au* 4 (2024): 3649–3656.

38. Y. Zou, M. Xue, W. Wang, et al., "One-ot Three-Enzyme Synthesis of UDP-Glc, UDP-Gal, and their Derivatives," *Carbohydrate Research*, 373 (2013): 76–81. https://doi.org/10.1016/j.carres.2013.03.005.

39. A. Pâris, T. Rundstadler, and P. Lafite, "Simultaneous One-Pot Multienzymatic Synthesis and Purification of Uridine-5′-Diphosphate-α-D-Glucuronide and Uridine-5′-Diphosphate-α-d-Xylose," *Carbohydrate Research*, 554 (2025): 109516. https://doi.org/10.1016/j.carres.2025.109516.

Supporting Information

Additional supporting information can be found online in the Supporting Information section.